Author Manuscript

Author Manuscript

Author Manuscript

Author Manuscript

HHS Public Access

Author manuscript

J Biomed Mater Res A. Author manuscript; available in PMC 2015 May 26.

Published in final edited form as:

J Biomed Mater Res A. 2014 May ; 102(5): 1325–1333. doi:10.1002/jbm.a.34791.

Tuning scaffold mechanics by laminating native extracellular matrix membranes and effects on early cellular remodeling

Salma Amensag and **Peter S. McFetridge**

J. Crayton Pruitt Family Department of Biomedical Engineering, University of Florida, Gainesville, Florida 32611-6131

Abstract

At approximately 50 μm thin, the human amniotic membrane (hAM) has been shown to be a versatile biomaterial with applications ranging from ocular transplants to skin and nerve regeneration. These investigations describe laminating layers of the hAM into a multilayered, conformation creating a thicker, more robust biomaterial for applications requiring more supportive structures. Amniotic membranes were decellularized using 4 M NaCl and prepared as either flat single-layered sheets or rolled into concentric five-layered configurations. Constructs were seeded with human vascular smooth muscle cells and cultured over 40 days to quantify biological and mechanical changes that occurred during early remodeling events. By day 40 single-layered constructs displayed a decreasing trend in cellular densities and glycosaminoglycan (GAG) concentration, comparative to multilayered constructs with increasing cell densities (from 9.1 to 32 × 10^6 cells/g) and GAG concentrations (from 6.07 to 17.4 mg/g). Oxygen diffusion was calculated and found to be sufficient to maintain cell populations through the constructs full thickness. Although an overall decrease in the modulus of elasticity was noted, the modulus in the failure range of rolled constructs stabilized at values 25 times higher than single-layered constructs. Rolled constructs typically displayed an upregulation of contractile and matrix remodeling markers (α-actin, SM22 and type 1 collagen, MMP-2 respectively) indicating biological adaptation. Considerable design flexibility can be achieved by varying the number of scaffold layers, allowing the possibility of tuning the constructs physical dimensions, shape and tensile properties to suit specific targeted vascular locations.

Keywords

tissue engineering; rolling approach; early remodeling

INTRODUCTION

Bioresorbable scaffolds provide a temporary biomechanical support during remodeling events until reseeded or endogenous cells produce their own extracellular matrix (and ideally) regain biological function.[1] When used as a 3D scaffold, *ex vivo* derived tissues

© 2013 WILEY PERIODICALS, INC.

Correspondence to: P. S. McFetridge; pmcfetridge@bme.ufl.edu.

Additional Supporting Information may be found in the online version of this article.

Author Manuscript Author Manuscript Author Manuscript Author Manuscript

have a number of inherent advantages as they provide a natural biological structure and function to potentially enhance regenerative processes. The human amniotic membrane (hAM) is a fetal-derived tissue that has a number of advantageous properties when used as a prepared biomaterial, including: biocompatibility, biostability, low-inflammatory response, low-immunogenicity, vasoactivity, thromboresistance, ability to remodel, and its wide availability.[2,3] Clinically the hAM has shown potential in a versatile range of applications when used as a crosslinked barrier matrix, as well as for ocular, skin and cartilage regeneration.[3–9]

Although current applications have focused on its use as single-layered membrane, the material has the potential to be fabricated into different shapes and thicknesses by layering multiple single sheets to generate a thicker more robust biomaterial. By varying the number of layers and structural layout (for example tubular *vs*. flat sheets) a wide range of constructs can be generated and comprehensively tuned to suit specific anatomical locations. The investigations herein focus on the cellular response when cultured within two different conformations of the hAM scaffold (hAMS): single-layered and multilayered laminate biomaterial, using an alternative salt-based decellularization approach with an application toward vascular scaffold design.

Extraction of soluble ECM components during decellularization differs as a function of the decellularization process,[10] and thus can directly influence the re-seeded cell's capacity to remodel the scaffold. Therefore, the removal of residual chemicals associated with decellularization is critical to minimize the potential for cytotoxicity[11,12] and maximize the potential for regeneration. In tissue engineering applications, including use of the hAM, the anionic surfactant sodium dodecyl sulfate (SDS) has been a commonly used chemistry to solubilize tissue components.[2,11–14] However, SDS is known to be cytotoxic and can disrupt the hydrogen bonding that stabilizes many of the larger insoluble ECM molecules, resulting in disruption of the collagen triple helix, swelling of the elastin network, and the removal of key adhesive proteins and glycosaminoglycans (GAG).[10,11,14,15] NaCl, by comparison, is a natural element present within the human body and as such is inherently less toxic. Further, due to its lower molecular weight SDS, NaCl is more effectively extracted from low porosity materials after treatment. Concentrated NaCl (4 *M*) generates an osmotic stress when incubated with *ex vivo* tissues, resulting in the solubilization of cell cytoplasmic components, and the disruption of nucleic acids which enables diffusion processes to extract these soluble components.[14–17]

In vascular tissue engineering, creating a medial layer equivalent is a key goal as it provides the main structural integrity of the vessel wall to allow sustained resistance to shear/tensile stresses associated with hydrostatic pressures.[18] In these investigations the early remodeling capacity of single and multilayered hAMS by smooth muscle cells (SMC) processed using a salt-based decellularization method was evaluated to assess biochemical, cellular and mechanical attributes for its potential use as a blood vessel substitute. Theoretical oxygen transport was calculated to determine limitations of supply over cell consumption rates due to inherently different transport conditions between flat and multilayered structures. Effects of the conformational change (flat *vs*. rolled) on SMC number, metabolic activity,

Author Manuscript Author Manuscript Author Manuscript Author Manuscript

extracellular matrix (ECM) secretion, as well as progressive biomechanical changes that contribute to vessel functionality were assessed over 40 days of culture.

MATERIAL AND METHODS

Isolation and decellularization of the hAM

Human amniotic membranes were isolated from placental tissues collected from the Woman's Delivery Center at the Norman Regional Hospital, Norman, OK, and the Shands hospital at the University of Florida, Gainesville, FL. The following bioscaffold decellularization steps were performed. Briefly, the amnion was manually separated from the chorion, then rinsed twice in deionized water and devitalized by two cycles of freezing/thawing, then agitated in 4 *M* NaCl at 100 rpm on an orbital shaker plate for 24 h. hAM were subsequently rinsed in successive solutions of deionized water, then incubated overnight at 37°C in 50 U/mL in a desoxyribonuclease (DNase) solution (Sigma, St. Louis, MO). After rinses in deionized water, samples were sterilized for 2 h in a 0.01% (v/v) peracetic and ethanol (2%, v/v) solution (Fluka, Switzerland). Samples were then pH balanced in PBS.

Cell culture and adhesion on bioscaffolds

Smooth muscle cells from ATCC (batch 2654) were expanded using Dulbecco's Modified Eagle's Medium (DMEM, Invitrogen, OR), supplemented with 1% penicillin-streptomycin (Gibco Life technologies, Grand Island, NY), and 10% of fetal serum complex (FetalPlex, Genimini Bio-Products, West Sacramento, CA). Cells were seeded as monocultures onto the stromal surface of hAM sections and stained with 4′-6-diamidino-2-phenylindole (DAPI stain, Invitrogen, OR) at a 300 n*M* concentration 2 h after seeding. A Carl Zeiss Axio Imager M2 Epifluorescent microscope (Göttingen, Germany) was used to identify cell nuclei on the surface of hAM.

Preparation and seeding of flat bioscaffolds

After decellularization sheets of hAM scaffold (hAMS) were dissected into 15 mm diameter disks (to fit standard six-well tissue culture plates (Corning, NY) and incubated in standard SMC cell culture media overnight at 37°C prior to seeding. SMC were seeded onto the stromal surface at a density of 600 cells/mm^2. Analyses were performed at days 0, 2, 4, 6, 10, 20, and 40.

Preparation and seeding of the rolled (multilayered) bioscaffolds

13 × 9 cm^2 rectangular sections were dissected from hAMS sheets and incubated in standard SMC culture media overnight at 37°C prior to seeding. SMC were seeded onto the flat sheets at a density of 600 cells/mm^2 and cultured for 10 days prior to rolling in the laminate structure. At day 10 reseeded hAMS were rolled five times around 4.2-mm diameter glass rod (stromal surface facing up) to form the layered structure. After creating the laminate structure at day 10, analyses were performed on days 20, 30, and 40 (from initial seeding).

Author Manuscript Author Manuscript Author Manuscript Author Manuscript

Cell proliferation, metabolic activity and GAG content

Papain (Spectrum, Gardena, CA) was used to digest the hAMS at a 125 μg/mL concentration for 24 h at 60°C. After centrifugation, the concentration of DNA per sample was quantified using the Quanti-iT PicoGreen assay (Invitrogen, Oregon, USA) by quantifying the DNA bound fluorescent marker. Samples were excited at 480 nm and the fluorescence emission intensity was measured at 520 nm. Intensity was then plotted *versus* DNA concentration as per manufacturer instructions. Alamar Blue assay kit (Invitrogen, Oregon, USA) was used to measure metabolic activity per cell against a calibration curve of the same cell lineage. GAG content was assessed using dimethylmethylene blue (Sigma Aldrich, St Louis MO) and calibrated using chondroitin sulfate as a standard. All measurement of cell and GAG concentrations are reported per gram of hydrated tissue.

Gene expression

MiVarna isolation kit (Ambion, Austin, TX) was used to isolate RNA from tissues and cDNA was synthesized from 2 mg of the total RNA using SuperScript VILO cDNA Synthesis Kit (Invitrogen). Primer sequences (Integrated DNA Technologies, IDT, Coralville, IA) used in this study were: human SM-α actin: forward primer: 5′-CATCACCAACTGGGACGA-3′, reverse primer: 5′-GGTGGGATGCTCTTCAGG-3′; SM22: forward primer: 5′-GGCAGCTTGGCAGTGACC-3′, reverse primer: 5′-TGGCTCTCTGTGAATTCCCTCT-3′; and collagen type I: forward primer: 5′-ATGTGGCCATCCAGCTGAC-3′, reverse primer: 5′-TCTTGCAGTGGTAGGTGATGTTCT-3′. Real time polymerase chain reactions (RT-PCR) were run using either BioRad CFX96 or CFX384 Real-Time systems with glyceraldehyde-3-phosphate dehydrogenase (GAPDH) used as an internal control. The amount of DNA immunoprecipitated was determined using Power SYBR green PCR master mix (SA Biosciences, Frederick, MD). Relative mRNA levels were calculated using the $2^{-\Delta\Delta Ct}$ method normalized to the expression level in basal culture conditions, and expressed as the fold difference relative to SMC controls cultured on T75 flasks.

Tensile testing

Flat single-layered hAMS were dissected into sections with a 5:1 (length: width) ratio then loaded using cyanoacrylate glue between two vertically parallel clamps of an Instron uniaxial testing rig (Model 5542 Norwood, MA with Version 2.14 software, Instron). 0.1 *N* preload preceded extension at 5 mm/min of tissues until failure. Bulk material engineering stress values were calculated by dividing load to initial cross-sectional area values of each sample (using an average thickness of 50 μm). Strain values were obtained by normalizing sample deformation to initial length. Using the same testing parameters rolled hAMS were cut into 5 mm wide ringlets and attached to the test rig using two stainless L-shaped hooks. The elastic modulus (EM) corresponds to stress/strain in the linear region prior to material failure, and physiological EM was assessed from 0.01 MPa (80 mmHg) to a maximum of 0.02 MPa (120 mmHg) corresponding to a low-strain region that reflects physiologic behavior in the human vasculature (physiologic range). The rupture strength corresponds to the maximum stress at sample rupture.

Author Manuscript Author Manuscript Author Manuscript Author Manuscript

SEM and Histology

Samples were fixed for SEM in 2.5% glutaraldehyde (Sigma, St Louis, MO), washed in PBS, incubated in a 1% osmium tetroxide (Acros Organics N.V., Fair Lawn, NJ) solution and progressively dehydrated in a series of graded ethanol solutions, prior CO_2 critical point drying (Autosamdri-814, Tousimis, Rockville, MD). Samples were then gold sputtered (Hummer IV) and analyzed using a JEOL LSM-880 SEM at 10 kV.

Hematoxylin and Eosin staining were performed to analyze 5 μm sections, imaged using a Carl Zeiss Axio Imager M2 epifluorescent microscope (Göttingen, Germany).

Calculated oxygen diffusivity through single and five-layered constructs

The availability of oxygen to cells in the innermost layers of the construct was estimated using the transmissibility of oxygen through a single layer of the hAMS, assumed to be similar to native amnion (derived by Yoshita et al.[19] and found to be 92.9×10^{-9} $mLO_2/s\ cm^2\ mmHg$), and secondly, the oxygen consumption rate per cell (estimated to be 0.15 fmol/min cell[11,20,21]). Measured oxygen pressure within the culture media was determined using a BioProfile 400 Nutrient Analyzer (Nova Biomedical, Waltham, MA) and found to be 180 mmHg.[22] Using the ideal gas equation: $PV = nRT$, the oxygen concentration in media was determined at 310.15 Kelvin and 101,325 Pascal. The volumetric consumption of oxygen by cells Q ($mol/m^3\ s$) was calculated using $Q = c \times q$, where c corresponds to the cell concentration (cell number/m^3) and q the average consumption of oxygen/cell (mol/cell s).[20] Thus, in this system it was important to quantify the transmissibility of oxygen through the hAM, the availability of oxygen within the media and the consumption rate of oxygen by the cellular populations. Form these data the transport of oxygen across the hAM (single or multilayered) was estimated.

Statistical analysis

Statistical analysis was performed using the two-way ANOVA method using SPSS version 16.0.2 with significant differences corresponding to a $p < 0.01$ (confidence level ≥99%). Unless otherwise stated, all data are presented as mean values ± standard deviation from at least three independent experiments ($n = 3$).

RESULTS

Gross morphology, structure, cell adhesion on the flat single-layered bioscaffold

The native amniotic membrane is has two distinct surfaces, the inner basement membrane (bm) that, during pregnancy is exposed to the amniotic fluid and a stromal surface (s) that is physiologically bound to the chorionic membrane [Fig. 1(A), dotted line indicates approximate separation line between the amnion and chorion]. After NaCl decellularization processes, the scaffold was free of observable cell remnants in either in histology sections or SEM images [Fig. 1(B–D)]. SEM assessment of the decellularized basement membrane displayed a smooth morphology [Fig. 1(B)] relative to the more amorphous and porous stromal surface [Fig. 1(C)]. DAPI stained SMC were shown to adhere on the stromal surface [Fig. 1(E)] and basement membrane of flat single-layered hAMS [Fig. 1(F)]. Having a

Author Manuscript Author Manuscript Author Manuscript Author Manuscript

higher surface area than the basement membrane, the stromal side was chosen as the surface for reseeding due to increased cell adhesion rates (data not shown).

Morphology, structure, cell adhesion on the rolled five-layered bioscaffold

Ten days after initial seeding constructs were rolled around a 4.2 mm OD mandrel with the stromal surface facing toward the lumen. Zip ties (3-mm width) were used secure end of the tubular construct, with the rolling process bringing the stromal and basement membrane surfaces into close proximity. Ten days after rolling (20 days post-seeding), constructs displayed a smooth tubular structure, Figure 2(A), with cell growth observed between discrete layers and on the neo-lumen, Figure 2(B). Overall, cells remained closely associated with the initial seeded surface, displaying limited migration into each discrete layer of the hAM scaffold. Evidence of newly secreted extracellular matrix forming between the existing layers is indicated with arrows on histology image Figure 2(C).

SMC proliferation and GAG synthesis

SMC were seeded at an initial density of 10×10^6 cells/g (600 cells/mm^2). By day 20, cell densities on flat constructs had increased significantly reaching 30×10^6 cells/g. Increased cell density was concomitant with a 15-fold decline in metabolic activity until day 20 at which point metabolic activity maintained a steady state [Fig. 3(A)]. Metabolic activity on rolled constructs decreased significantly from day 20–40, whereas cell density increased significantly from 10 to 32 million of cells/g [Fig. 3(B)].

GAG concentrations within flat constructs reached maximum values of 16.9 mg GAG/g by day 10 then decreased to 14.1 mg GAG/g of tissue at day 20 [Fig. 4(A)]. Significant increases in both cell density and GAG concentrations were noted with the rolled constructs from day 20–40 (rolled on day 10 post-seeding), with a threefold increase in cell density and fivefold increase in GAG concentration [Fig. 4(B)].

Cell phenotype

Expression of SMC phenotypic markers (α-actin, SM22) and ECM remodeling activity (type 1 collagen and MMP-2) were assessed on single membranes at day 10, and on rolled multilaminate scaffolds (five-layers) 20 and 40 days post-seeding. Cells cultured on standard tissue culture plastic served as controls. A significant up regulation of α-actin, SM22, type 1 collagen and MMP2 was observed with rolled constructs (day 20) compared to flat constructs at day 10. The contractile SMC markers α-actin and SM22 were up regulated at day 20 (rolled), however 30 days after the constructs were rolled; all genes reached values similar to the initial values as seen on the flat single-layered constructs at day 10 (Fig. 5).

Biomechanical properties

Variations in the constructs modulus of elasticity were evaluated over the full culture period and assessed in both the failure and physiological ranges, as shown in Figure 6(A,B). Physiological moduli decreased by a factor of 10 from flat single-layered constructs (0.1 MPa) to rolled hAMS (0.01 MPa) by day 40. In the failure range the rolled five-layered scaffolds were shown to have modulus values nine times higher than single-layered hAMS. By comparison to the single-layered hAMS that displayed a single failure point, the rolled

Author Manuscript Author Manuscript Author Manuscript Author Manuscript

constructs displayed three distinct fracture points that were associated with each layer failing during extension, illustrated by the arrows Figure 6(C).

Figure 7 displays the rupture stress of flat (A) and rolled (B) constructs. After a progressive increase from 0.6 MPa at day 2–2.1 MPa at day 10, the rupture strength of flat constructs declined reaching statistically similar values from day 30 until termination at day 40. Rolled constructs displayed a significant increase in rupture stress at day 20 (10 days post-rolling) relative to single-layered constructs, which was then followed by a reduction between days 30–40. Despite a significant reduction in stress forces (rolled constructs) to 0.3 MPa at day 40, these values were significantly higher than flat constructs at 0.09 MPa. Rolled "acellular" controls were not possible as the binding of adjacent hAM layers was a "cell-dependent" process, as such scaffolds unwound either during incubation or tensile testing, and did not provide useful information.

Oxygen diffusion

Factors determining the availability of oxygen to cells in either single, or five-layered configurations are reported Table 1. These key parameters include; the quantity of oxygen available in the initial media supply, the innate transmissibility of oxygen through the hAMS, and the derived cell concentrations and oxygen consumption rates.[11,19–21,23]

Knowing initial oxygen transmissibility of the scaffold, and oxygen concentration in media (derived from the ideal gas equation to be 9.31 mol/L), oxygen transport through a single layer of hAMS (23.4 cm^2) was estimated to be 0.391 $\mu LO_2/s$, and through the five hAM layers to be 16.5×10^{-6} mLO_2/cm^2 s,[19,24] an order of magnitude higher than the diffusion constant of the native human arteriole wall (approximately 1×10^{-6} mLO_2/cm^2 s[23]).

At day 20 (10 days post-rolling), cell concentrations within the laminated construct reached 10 million cells/g of tissue. The oxygen consumption rate of vascular SMC was previously found to be 0.15 fmol/min cell.[21] Thus, the volumetric consumption of oxygen by cells within one hAMS layer is 2.1 nmol/min. Cells consumed a total of 6.49 mL of oxygen, corresponding to 0.0605 mol/L over the 20 day culture period.

Knowing the transmissibility of oxygen through the hAM and the cellular consumption rate (after 20 days culture), a total oxygen concentration of 61.01 mL (single layer) and 35.13 mL (five layers) was available to cells in this system, which was significantly more than the 6.49 mL of oxygen required for maintenance of the total cell population.[11,20,21]

DISCUSSION

This study reports the early remodeling activity of an *ex vivo* derived material as a function of its conformation (flat or multilaminate) for tissue engineering applications. Using this multilayer approach the material has the potential to be mechanically tuned to suit specific mechanical and geometric requirements associated with various anatomical locations. In this study, we assessed the hAM as a multilayer tubular construct that can be readily rolled into a tubular structure for blood vessel regeneration. Our hypothesis was that its rolled

Author Manuscript Author Manuscript Author Manuscript Author Manuscript

conformation compared to the flat geometry would more closely resemble the natural 3D structure and *in vivo* environment resulting in improved remodeling processes.

The hAM has been decellularized using a variety of different physical and chemical methods.[7,12,25–28] Among the commonly used approaches is the ionic surfactant SDS,[2,12,13] however the mechanism with which SDS decellularizes tissues is aggressive, as it strips GAG's, damages collagen fibers, and disrupts the biological and mechanical proprieties of the native tissue. As such decellularization treatments affect adhesion of reseeded cells, their migration, metabolic activity and growth, eventually resulting in suboptimal remodeling that may inhibit regenerative processes.[12] To reduce these adverse ECM interactions a less aggressive approach to decellularize the tissue was used, based on a hypertonic NaCl solution to destabilize and remove cellular components.[14] These investigations support previous studies showing the NaCl treatment to be effective at removing cellular components from the native hAM.[14–17] Material surfaces were clear of cellular debris, as seen with SEM and histological images, showing no sign of intact cell bodies within the bulk material, again supporting previous studies. The acellular scaffold maintained its cells adhesion properties as noted by adhesion of reseeded SMC and EC [Fig. 1(E) and Supporting Information Figure SA/B). SEM images show the stromal surface, composed predominantly of type 1 collagen, to have a more porous surface relative to the type IV collagen basement membrane (BM) that displayed a smoother, more uniform structure. Each of these morphologies would likely interact differentially with specific cell types and influence cell function accordingly. For example, the hAM's BM structure, morphology and composition resembles the lumenal surface of blood vessels and was hypothesized to be better suited for endothelial cells adhesion and function, relative to the more porous stromal surface (that maybe better suited to smooth muscle cell function). However, further investigations are required to evaluate this hypothesis.

The change of scaffold conformation from flat membrane into the multilaminate conformation 10 days after seeding brought the SMC seeded on the stromal surface into close proximity to the BM. Subsequent to the rolling process, cell densities and GAG concentration reduced, an effect due to the procedure itself, where the hydrate GAG/cell rich layers were compressed and (effectively) squeezed from the matrix surface. However, this was followed by increased cell concentrations between days 20 and 30 (post-rolling) as well as significant and concomitant increase in GAG concentrations. Early scaffold remodeling was evident in histology images showing interactions between adjacent layers as cells increased in density and synthesized ECM components, including GAG. While these investigations focused on generating the vascular medial layer, a preliminary assessment of endothelial cell (EC) and EC/SMC co-cultures was completed to confirm the membranes potential to develop a complete functional vessel as part of future directions, see Supporting Information Figure SA/B.

Tensile data indicated the discrete layers of the laminated constructs to initiate binding, forming a relatively uniform tubular material. This resulted in an extended failure profile relative to load values of single-layered membranes, see Figure 6(C). Interestingly, while the GAG concentrations increased, expression of type 1 collagen decreased significantly with a concomitant reduction in rupture strength. Despite the drop of mechanical strength, the

Author Manuscript Author Manuscript Author Manuscript Author Manuscript

hAMS constructs stabilized over the last 10 days of culture and maintained adequate rupture strength for blood vessel applications. One of the advantages of using natural materials is the maintenance of the vessels viscoelastic properties, particularly over the physiological operating range, which conferred by its elastin and collagen composition.[29] Indeed, unlike many engineered vessels particularly those using synthetic materials that have little or no elastin content,[29,30] the hAM amongst other fundamental ECM molecules incorporate similar content of elastin than naturally occurring BV (490.8 μg/mg[12]). Thus, the mechanical stability and elastic profile of this construct may be attributed to the high elastin content of the native hAMS. In addition to large elastin quantity within the hAM, 0.049% of matrix hydroxyproline, 0.085% of GAG, 0.001% of denatured collagen were quantified in the hAM, all critical ECM molecule for scaffold regeneration.

Although structural and cellular microenvironments within the hAM differ considerably from one conformation (flat) to the other (rolled), the material's initial biological and mechanical properties remain similar. Compared to the 2D nature of the flat material, mass transfer limitations due to the enclosed structure of the rolled configuration where hypothesized to inhibit cell function due to nutrient deprivation. Conversely, the enclosed structure may promote a more mature phenotype due to cells being encased within an ECM structure that more closely resembles natural tissue. As a preliminary validation study, oxygen availability was calculated through single and five-layered constructs and found to be 67.6 and 35.13 mL respectively, with an estimated consumption rate by human vascular smooth muscle cells to be 0.15 fmol/min cell.[11,20,21] Based on these calculations, cell concentrations at day 20, that displayed similar densities to native vessels (70 million cells/g), were not limited by oxygen availability.[19,24] Diffusion of oxygen through the hAM was shown to be in the same order of magnitude as native vessels.[19,24] Oxygen diffusion gradients are strongly influenced by changing cell densities where an increasing population will consume more oxygen, generating a steeper gradient; as reported by a recent study were collagen-based structures were used to identify relationships between oxygen and cell density.[31] Following these theoretical calculations, the limiting number of hAM layers to support the cell density in this system would be nine layers (corresponding to an approximate thickness of 450 μm). Nevertheless, sufficient oxygen diffusivity in a complex remodeling environment is dynamic and ultimately dependent on the final cell densities, their consumption rate, and changing diffusivity due to ECM remodeling. Future investigations using pulsatile perfusion conditions with controlled transmural pressure drop/flow will enhance nutrient delivery by increasing the pressure gradient and improving mass transport conditions across the scaffold wall. This in effect would potentially allow scaffolds with more than nine layers to be used without oxygen deprivation.

By comparison to the multilayered constructs, the single-layered scaffold displayed significant early remodeling up to day 20 before reaching a more stable state with declining cell densities. By comparison, cell densities and GAG content on the multilayered constructs initially decreased then displayed a significant increase up to day 40 (experimental termination) that is indicative of sustained remodeling. From a broader perspective, the rolled conformation compared to the flat geometry more closely resembles the natural *in vivo* 3D environment and was hypothesized to create a *milieu* that would enhance

Author Manuscript Author Manuscript Author Manuscript Author Manuscript

remodeling capabilities. In this study, cells remained closely associated with the initial seeded surface, displaying limited migration into each discrete layer of the hAM scaffold. Tosun et al.[32] showed constructs cultured under dynamic conditions with an applied physiologically modeled pressure-drop (transmural) to display enhanced cell migration and dispersion through *ex vivo* derived scaffolds. As such, as part of our future work, we will assess the early remodeling events of the rolled hAMS cultured under pulsatile perfusion conditions (with a transmural pressure drop of 120 mmHg (max) 80 mmHg (min). Compared to previously reported work[13] where the hAMS was prepared using the surfactant SDS, the NaCl treatment used herein resulted in a qualitative increase in porosity of the basement membrane.[13] This variation would likely influence cell function as transport conditions vary. Overall both the single and multilayered bioscaffolds decellularized with NaCl resulted in SMC displaying an increased proliferative capacity (threefold increase in cell density), migration, and GAG synthesis.[13] The observed increased bulk mechanical properties of the five-layered constructs relative to the single-layered hAMS was hypothesized to be a function of early ECM synthesis and remodeling events fusing layers together in a binding process.

A limitation of many *ex vivo* tissues when used as implant materials is being tied to a specific geometry, which limits their respective applications. By using this multilaminate design, scaffolds have the potential to be engineered to suit specific anatomical locations where shape, diameter, length and thickness of the final constructs can be tailored. Rolled conformation provides a 3D environment that resemble natural arteries, where seeded cells where shown to displayed an enhanced early remodeling compared to the flat geometry. Further, by using a developed ECM with predicable mechanical function the potential exists to reduce the regenerative time span to create functional materials. Thus, this combined cell-dense ECM rolling method and *ex vivo* scaffold provides a promising approach to develop engineered tissues in clinically relevant time frames.

Supplementary Material

Refer to Web version on PubMed Central for supplementary material.

REFERENCES

1. Schenke-Layland K, Vasilevski O, Opitz F, König K, Riemann I, Halbhuber KJ, Wahlers T, Stock UA. Impact of decellularization of xenogeneic tissue on extracellular matrix integrity for tissue engineering of heart valves. J Struct Biol. 2003; 143:201–208. [PubMed: 14572475]
2. Niknejad H, Peirovi H, Jorjani M, Ahmadiani A, Ghanavi J, Seifalian AM. Properties of the amniotic membrane for potential use in tissue engineering. Eur Cell Mater. 2008; 15:88–99. [PubMed: 18446690]
3. Niknejad H, Peirovi H, Jorjani M, Ahmadiani A, Ghanavi J, Seifalian AM. Properties of the amniotic membrane for potential use in tissue engineering. Eur Cell Mater. 2008; 15:88–99. [PubMed: 18446690]
4. Kheirkhah A, Johnson DA, Paranjpe DR, Raju VK, Casas V, Tseng SC. Temporary sutureless amniotic membrane patch for acute alkaline burns. Arch Ophthalmol. 2008; 126:1059–1066. [PubMed: 18695099]
5. Maharajan VS, Shanmuganathan V, Currie A, Hopkinson A, Powell-Richards A, Dua HS. Amniotic membrane transplantation for ocular surface reconstruction: Indications and outcomes. Clin Exp Ophthalmol. 2007; 35:140–147.

Author Manuscript Author Manuscript Author Manuscript Author Manuscript

6. Tamhane A, Vajpayee RB, Biswas NR, Pandey RM, Sharma N, Titiyal JS, Tandon R. Evaluation of amniotic membrane transplantation as an adjunct to medical therapy as compared with medical therapy alone in acute ocular burns. Ophthalmology. 2005; 112:1963–1969. [PubMed: 16198422]
7. Jin CZ, Park SR, Choi BH, Lee KY, Kang CK, Min BH. Human amniotic membrane as a delivery matrix for articular cartilage repair. Tissue Eng. 2007; 13:693–702. [PubMed: 17269856]
8. Mligiliche N, Endo K, Okamoto K, Fujimoto E, Ide C. Extracellular matrix of human amnion manufactured into tubes as conduits for peripheral nerve regeneration. J Biomed Mater Res. 2002; 63:591–600. [PubMed: 12209905]
9. Mohammad J, Shenaq J, Rabinovsky E, Shenaq S. Modulation of peripheral nerve regeneration: A tissue-engineering approach. The role of amnion tube nerve conduit across a 1-centimeter nerve gap. Plastic Reconstruct Surg. 2000; 105:660–666.
10. Rieder E, Kasimir M-T, Silberhumer G, Seebacher G, Wolner E, Simon P, Weigel G. Decellularization protocols of porcine heart valves differ importantly in efficiency of cell removal and susceptibility of the matrix to recellularization with human vascular cells. J Thorac Cardiovasc Surg. 2004; 127:399–405. [PubMed: 14762347]
11. Gilbert TW, Sellaro TL, Badylak SF. Decellularization of tissues and organs. Biomaterials. 2006; 27:3675–3683. [PubMed: 16519932]
12. Wilshaw SP, Kearney JN, Fisher J, Ingham E. Production of an acellular amniotic membrane matrix for use in tissue engineering. Tissue Eng. 2006; 12:2117–2129. [PubMed: 16968153]
13. Amensag S, McFetridge PS. Rolling the human amnion to engineer laminated vascular tissues. Tissue Eng Part C Methods. 2012; 18:903–12. [PubMed: 22616610]
14. Kim WG, Park JK, Lee WY. Tissue-engineered heart valve leaflets: An effective method of obtaining acellularized valve xenografts. Int J Artif Organs. 2002; 25:791–797. [PubMed: 12296464]
15. Uzarski JS, Van De Walle AB, McFetridge PS. Preimplantation processing of ex vivo-derived vascular biomaterials: Effects on peripheral cell adhesion. J Biomed Mater Res A. 2013; 101:123–131. [PubMed: 22825780]
16. Xu CC, Chan RW, Tirunagari N. A biodegradable, acellular xenogeneic scaffold for regeneration of the vocal fold lamina propria. Tissue Eng. 2007; 13:551–566. [PubMed: 17518602]
17. McFetridge PS, Abe K, Horrocks M, Chaudhuri JB. Vascular tissue engineering: Bioreactor design considerations for extended culture of primary human vascular smooth muscle cells. ASAIO J. 2007; 53:623–630. [PubMed: 17885337]
18. Wagenseil JE, Mecham RP. Vascular extracellular matrix and arterial mechanics. Physiol Rev. 2009; 89:957–989. [PubMed: 19584318]
19. Yoshita T, Kobayashi A, Sugiyama K, Tseng SC. Oxygen permeability of amniotic membrane and actual tear oxygen tension beneath amniotic membrane patch. Am J Ophthalmol. 2004; 138:486–487. [PubMed: 15364239]
20. Lovett M, Lee K, Edwards A, Kaplan DL. Vascularization strategies for tissue engineering. Tissue Eng Part B Rev. 2009; 15:353–370. [PubMed: 19496677]
21. Guarino RD, Dike LE, Haq TA, Rowley JA, Pitner JB, Timmins MR. Method for determining oxygen consumption rates of static cultures from microplate measurements of pericellular dissolved oxygen concentration. Biotechnol Bioeng. 2004; 86:775–787. [PubMed: 15162453]
22. Moore M, Sarntinoranont M, McFetridge P. Mass transfer trends occurring in engineered ex vivo tissue scaffolds. J Biomed Mater Res A. 2012; 100:2194–2203. [PubMed: 22623220]
23. Vadapalli A, Pittman RN, Popel AS. Estimating oxygen transport resistance of the microvascular wall. Am J Physiol Heart Circ Physiol. 2000; 279:H657–H671. [PubMed: 10924065]
24. Porta M, Capurro C, Parisi M. Water permeability in the human amnion: Ph regulation of the paracellular pathway. Biochim Biophys Acta. 1989; 980:220–224. [PubMed: 2930789]
25. Koizumi N, Rigby H, Fullwood NJ, Kawasaki S, Tanioka H, Koizumi K, Kociok N, Joussen AM, Kinoshita S. Comparison of intact and denuded amniotic membrane as a substrate for cell-suspension culture of human limbal epithelial cells. Graefes Arch Clin Exp Ophthalmol. 2007; 245:123–134. [PubMed: 16612639]
26. Lim LS, Riau A, Poh R, Tan DT, Beuerman RW, Mehta JS. Effect of dispase denudation on amniotic membrane. Mol Vis. 2009; 15:1962–1970. [PubMed: 19784395]

Author Manuscript Author Manuscript Author Manuscript Author Manuscript

27. Portmann-Lanz CB, Ochsenbein-Kolble N, Marquardt K, Luthi U, Zisch A, Zimmermann R. Manufacture of a cell-free amnion matrix scaffold that supports amnion cell outgrowth in vitro. Placenta. 2007; 28:6–13. [PubMed: 16516964]

28. Wilshaw SP, Kearney J, Fisher J, Ingham E. Biocompatibility and potential of acellular human amniotic membrane to support the attachment and proliferation of allogeneic cells. Tissue Eng Part A. 2008; 14:463–472. [PubMed: 18370928]

29. Patel A, Fine B, Sandig M, Mequanint K. Elastin biosynthesis: The missing link in tissue-engineered blood vessels. Cardiovasc Res; 2006; 71:40–49.

30. Seliktar D, Nerem RM, Galis ZS. Mechanical strain-stimulated remodeling of tissue-engineered blood vessel constructs. Tissue Eng. 2003; 9:657–666. [PubMed: 13678444]

31. Cheema U, Hadjipanayi E, Tammi N, Alp B, Mudera V, Brown RA. Identification of key factors in deep o2 cell perfusion for vascular tissue engineering. Int J Artif Org. 2009; 32:318–328.

32. Tosun Z, McFetridge PS. Improved recellularization of ex vivo vascular scaffolds using directed transport gradients to modulate ecm remodeling. Biotechnol Bioeng. 2013; 110:2035–2045. [PubMed: 23613430]

Author Manuscript Author Manuscript Author Manuscript Author Manuscript

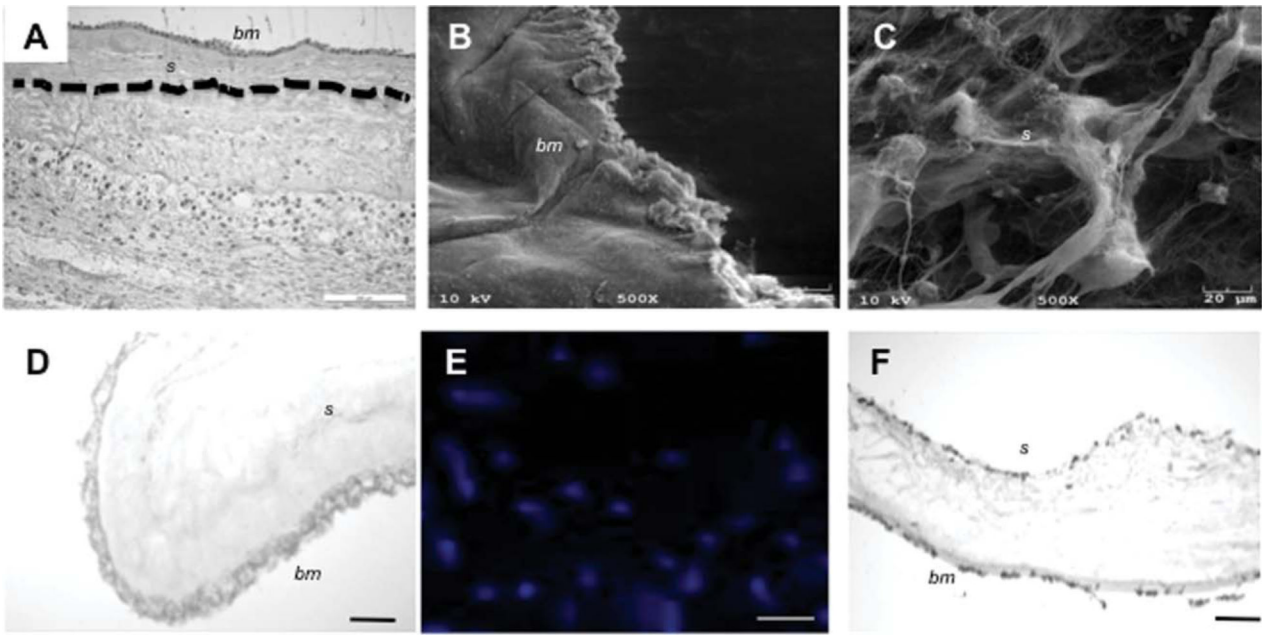

FIGURE 1.

Morphology and structure human amnion (single layer). Histology of the native placental membrane highlights its multilayer structure (the amnion/chorion separation is highlighted by a dotted line) (A). SEM surface analysis illustrates the topography of the decellularized hAM basement membrane (epithelial surface) (B) showing a uniform structure with a less porous morphology relative to the stromal surface (C). Histology (D) of the processed hAM confirmed the absence of cell remnants after 4M NaCl decellularization treatments. SMC seeded on the stromal surface were shown to adhere and proliferate of cell seeding as seen on DAPI results (E) and histology (F). Similarly, 2h post-seeding ECs adhered to the stromal surface of the hAM (F). Scale bar = 200 μm (A), 20 μm for SEM (B/C) and 50 μm (D/E/F). [Color figure can be viewed in the online issue, which is available at wileyonlinelibrary.com.]

Author Manuscript Author Manuscript Author Manuscript Author Manuscript

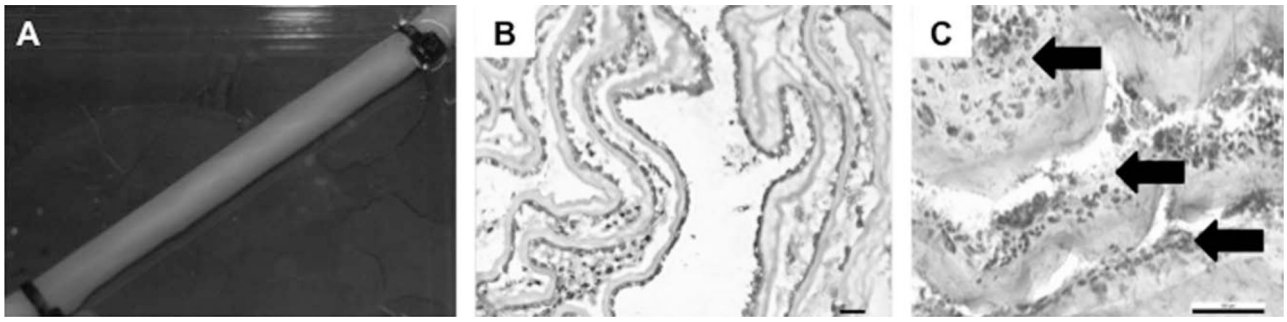

FIGURE 2.

The human amnion as a rolled conduit. Ten days after cell seeding, the flat hAM was rolled to form a tubular fivelayered conduit (A). By day 20, cell growth between different layers was observed (B and C) as well as deposition of newly synthesized ECM, as distinguished from native ECM shown by the black arrows (C). Scale bar 5 50 μm (B/C).

Author Manuscript
Author Manuscript
Author Manuscript
Author Manuscript

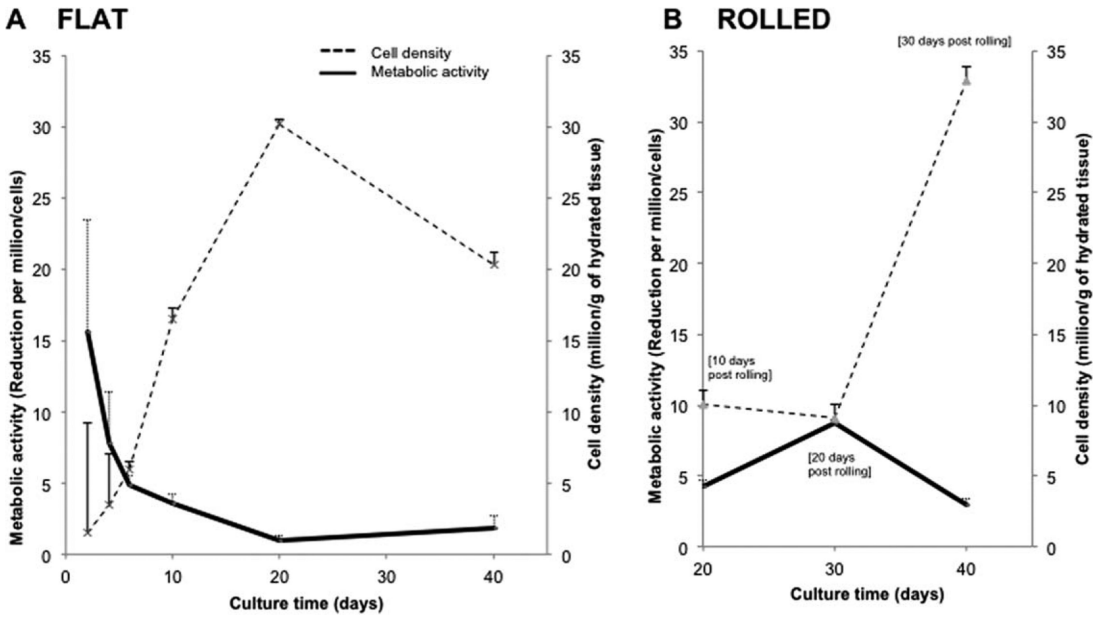

FIGURE 3.

Vascular SMC density and metabolic activity on single and multilayered constructs. Exponential cell proliferation was noted on the flat constructs by day 10 followed by a decrease from day 20–40. Conversely, metabolic activity displayed a progressive decrease over the same period (A). Rolled constructs by comparison progressively increased in cell density while no statistical difference in metabolic activity was noted over the culture period (B) ($n = 3$).

Author Manuscript Author Manuscript Author Manuscript Author Manuscript

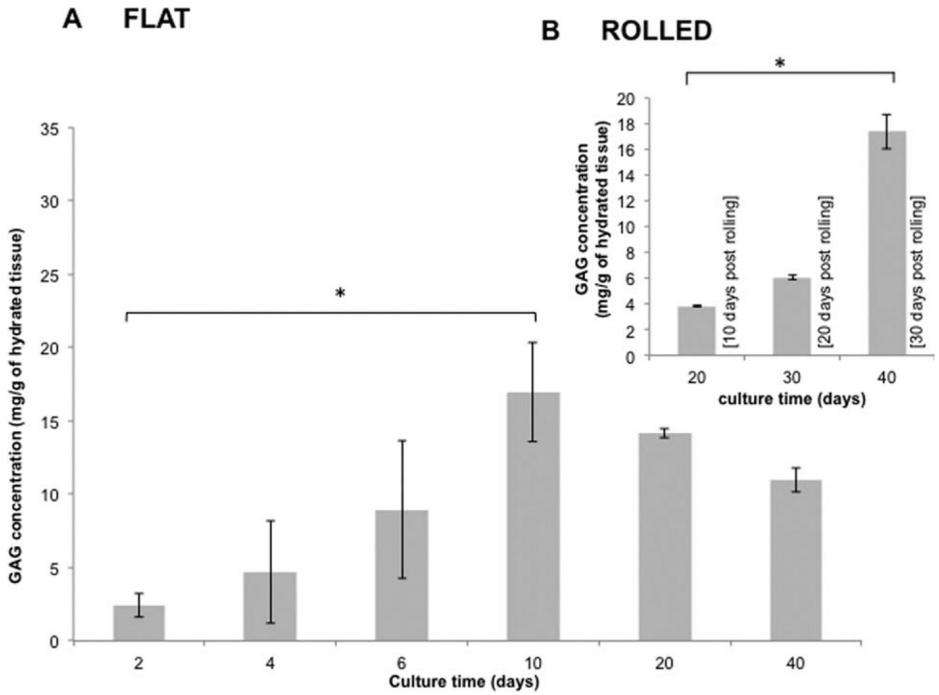

FIGURE 4.

Glycosaminoglycan concentration. A progressive synthesis of GAG was observed until day 10 reaching a concentration of 17 mg of GAG/g of hydrated construct, with no significant statistical difference thereafter until day 40. Rolled constructs increased GAG concentrations from day 20 at 4 mg to 17 mg of GAG/g of hydrated tissue by day 40 (B) (n = 9).

Author Manuscript Author Manuscript Author Manuscript Author Manuscript

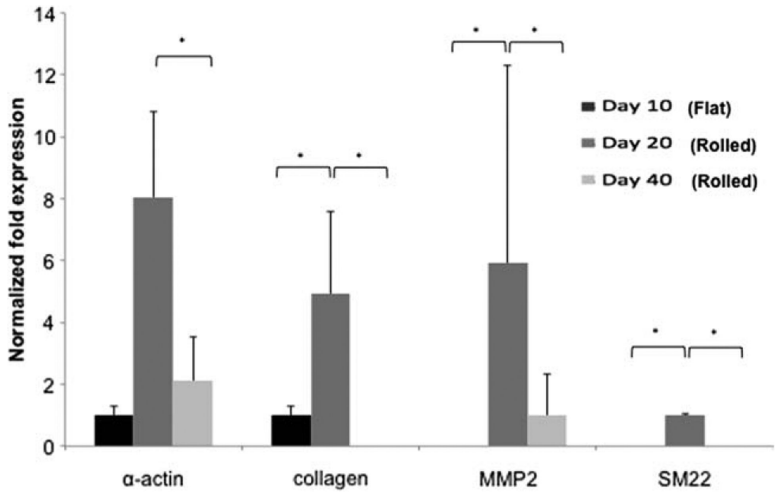

FIGURE 5.

SMC gene expression. RT-PCR expression analysis was performed on flat constructs at day 10 and on rolled constructs at days 20, and 40. Fold differences expression profiles were calculated using the $2^{-\Delta\Delta Ct}$ method and normalized to expression levels of SMC cultured under basal culture conditions (controls). At day 20 (rolled bioscaffolds) all genes had higher levels of expression compared to controls, day 10 (flat) and day 40 (20 days after rolling process).

Author Manuscript Author Manuscript Author Manuscript Author Manuscript

A

Flat hAM

	Control	Day 2	Day 4	Day 6	Day 8	Day 10	Day 20	Day 30	Day 40
Modulus, physiological range (MPa)	0.22	0.14	0.07	0.28	0.26	0.24	0.13	0.22	0.14
	±0.05	±0.03	±0.02	±0.06	±0.03	±0.1	±0.01	±0	±0.01
Modulus, failure range (MPa)	9.1	7.2	2.0	4.8	8.8	11.6	3.1	0.8	0.2
	±2.0	±4.7	±0.7	±1.9	±2.3	±2.7	±1.0	±0.5	±0.1

B

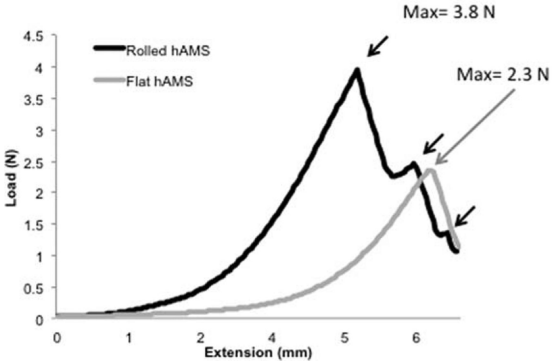

C

Rolled hAM

	Day 20	Day 30	Day 40
Modulus, physiological range (MPa)	0.05	0.001	0.01
	±0.03	±0	±0.01
Modulus, failure range (MPa)	28.1	5.3	4.7
	±5.3	±5.1	±3.2

FIGURE 6.

Physiological and failure elastic modulus properties of the hAMS in flat single layered and rolled conformations. Tables of modulus of elasticity variations over the failure range (prior rupture) and physiological range (from 80 to 120 mmHg) of flat single-layered and rolled constructs are given (A) and (B), respectively. On the failure profile, flat hAMS displayed a single fracture point at 2.3 *N* compared to the three fractures point observed on the rolled configurations at 3.8 *N* ($n = 5$), see (C). *$p < 0.01$.

Author Manuscript Author Manuscript Author Manuscript Author Manuscript

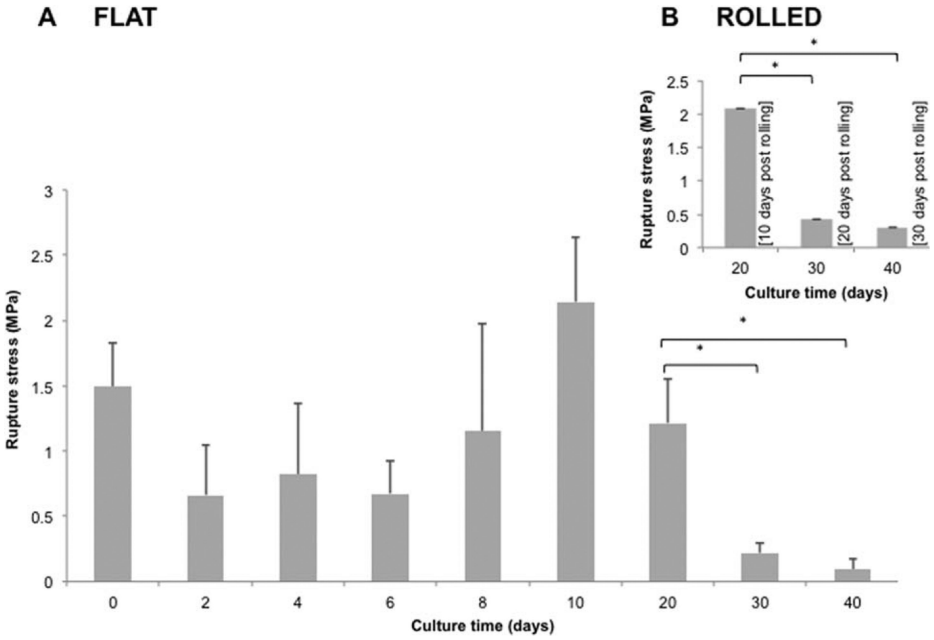

FIGURE 7.

Rupture stress of the hAMS. Profile of tensile rupture of the construct within time is given for flat and rolled conformations.

Author Manuscript

Author Manuscript

Author Manuscript

Author Manuscript

TABLE 1

Oxygen Diffusion: Factors Determining the Availability of Oxygen to Cells in Either Single, or Five-Layered Configurations

	1 Layer	5 Layers
Material thickness (μm)[1,2]	50	250
Number of cells within hAMS at day 20 (million)	14	70
Calculated oxygen consumption by cells (mL)	6.49	32.47
Calculated volumetric consumption of oxygen by cells (nmol/min)	2.1	10.5
Oxygen transmissibility (immersed in media) (μL O_2/s)	0.391	1.955
Oxygen that diffused seeded layer(s) (immersed in media) (mL)	61.01	35.13